Inorganic Chemistry

pubs.acs.org/IC

Article

Expanding the Concepts Trans Influence and Back-Donation: Hybrid and Side Donations in [Cp*M^{III}(L)XY] (M = Rh, Ir) Complexes with CO, CN$^-$, and CNR Ligands. A Window to Cis Influence

Sara Fernández-Moyano, Marconi N. Peñas-Defrutos,* Camino Bartolomé,* and Pablo Espinet*

Cite This: *Inorg. Chem.* 2021, 60, 14410−14417

Read Online

ACCESS | Metrics & More | Article Recommendations | Supporting Information

ABSTRACT: Analysis of the bonding contributions in molecules [M^{III}Cp*(L)XY] (M = Rh, Ir; Cp* = C_5Me_5; L = CO, CN$^-$, CNR) has uncovered a rich variety of types of interaction that seem to have escaped detection so far, in spite of the continuous popularity of cyclopentadienyl transition-metal complexes since the 1970s. At variance with the M—C≡O bond in square-planar systems, which shows typical metal-to-CO π-back-donation, the nonorthogonal arrangement of the Cp* plane and Rh—C≡O fragment and the pseudooctahedral geometry lead to the observation of many direct lateral donations from other ligands that do not involve the metal orbitals, and we name side donations, for instance, Cp* → π*(CO), Cl → π*(CO), and F → π*(CO). Hybrid donations partially involving the metal, M−C_{aryl} → π*(CO), are also observed. The summation of multiple contributions other than back-donation can easily account for about 20% of the electron donation to the π*(C≡O) orbitals.

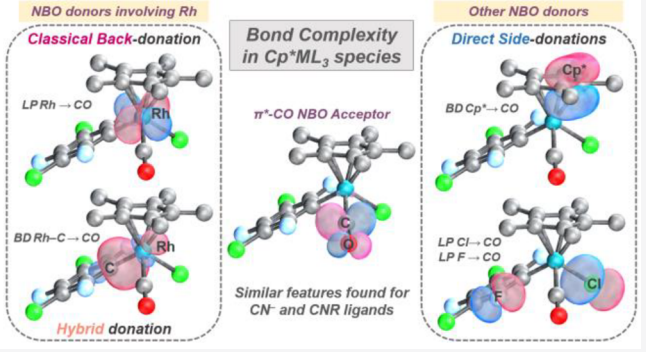

INTRODUCTION

Classic studies of the kinetic and structural effects of ligands coordinated to a metal started with the seminal studies of Chernyaev on square-planar platinum(II) complexes[1] and were lucidly discussed long ago by Hartley.[2] The basic concepts and rules developed are now textbook knowledge collected in Inorganic Chemistry books, but their use and understanding are not always free of errors or undefinitions. The two main concepts involved in d^n square-planar complexes are trans influence, associated with ground-state properties, and trans effect, in which ground and transition states are involved. Consequently, the trans influence is a thermodynamic effect determined by enthalpy changes and can be physically observed as variations of the bond distances, bond strengths, coupling constants, or vibrational wavenumbers. The trans effect is determined by the free energy difference between the ground and transition states and produces observable kinetic effects. The ligands are classified in a hopefully useful series by their trans influence or their trans effect on other ligands in the trans position. The studies were carried out on σ ligands, square-planar complexes, and d^n metal centers, but the results obtained are sometimes extrapolated to other geometries. Obviously, the series initially established on the experimental basis of d^n square-planar structures cannot be expected to apply accurately to any geometry (particularly those where the cis influence can be important), to main group or f^n elements, to ligand-substitution mechanism changes, or to molecules with side-bonded ligands (e.g., H−H or olefins). In fact, the different orbitals involved in bond interactions are determinant for the ligand−ligand and metal−ligand mutual influences.[3−5]

When the matter is restricted to the cases of d^n transition metals and the more common trans-influence series available, there are three cases that we want to consider (Figure 1). For ligands that interact through σ bonds, the stronger donors (e.g., L^1) polarize the electron density of the metal bond toward the weaker donor in the trans position (e.g., L), producing M−L bond elongation and making the L ligand weaker toward heterolytic dissociation.[6] "The more donor L^1,

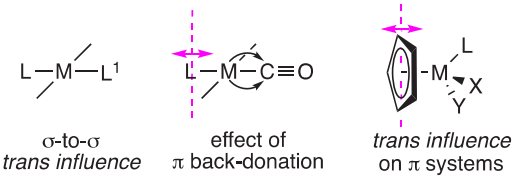

Figure 1. Three cases of trans influence in molecules.

Received: July 20, 2021
Published: September 9, 2021

https://doi.org/10.1021/acs.inorgchem.1c02189
Inorg. Chem. 2021, 60, 14410−14417

the higher M−L bond elongation" defines well the order of the trans influence of these ligands in the series (Figure 1, left). This ligand influence can be extrapolated relatively safely to other geometries.

There are two archetypical examples of complication for the ligand position in a trans-influence series. In both cases, the origin of the problem is the substantial implication of π orbitals. For the case of the end-coordinating π-acceptor CO ligand as the influencer ligand, it is known that free CO is a very bad donor, but in M−CO bonds, there is an important π-back-donation component, with a synergistic π/σ effect that strengthens the M−CO bond and weakens the M−L bond (Figure 1, middle). Because this back-donation depends on factors such as the energy of the d orbitals, the oxidation state of M, and others, the CO ligand is wandering in the different trans-influence series at reach in books, although it often appears in positions typical of fairly strong donors when the series is based on X-ray M−L bond distances. Theoretical analysis of the σ-donation and π-back-donation in CO complexes continues to be an active research subject as new methods appear.[7]

The other very frequent complicated case, that of side-on-bonded olefins and aromatic systems, is represented here by a pseudooctahedral [CpM(L)XY] complex (Figure 1, right). At variance with formal octahedral complexes, we cannot define three Cp−M bonds being influenced by the three M−L^n bonds that are trans to them. In a recent paper on Cp*Rh^{III} complexes (Cp* = C_5Me_5), we decided to use the Cp*$_{centroid}$−M distance data from X-ray studies as an average measure to study the trans influence of the other ligands on the Cp*M interaction. With this simplification, we could show that this distance breathes quite markedly depending on the donor strength of the other ligands: the dominant π nature of the Cp* electron density involved in this bond donation to the metal is particularly sensitive to trans influence by the other ligands. In fact, by changing the Cp*$_{centroid}$−M distance, the Cp*M interaction attenuates the influence of the other ligands on the rhodium(III) electron density. We named this remarkable feature the *electronic buffer effect* of Cp*.[8]

In this work, we focus our study on the latter two cases of Figure 1 [including now iridium(III) compounds] and show that, on complexes with strongly accepting CO- or CN-containing ligands, the role of Cp* or other potential donors in the other ligands is more complex than analyzed so far. The effects discussed here for second- and third-row transition metals should be even more marked in first-row CpM complexes (nowadays very used catalysis), where the Cp−M bond distances are shorter.

RESULTS AND DISCUSSION

Synthesis of RhCp*(a) and IrCp* (b) Complexes Bearing the Fluorinated Aryl 3,5-$Cl_2C_6F_3$ (Rf). These syntheses are depicted in Scheme 1. Because the chemistry of the Cp*Ir complexes in this work is so similar to the one we previously reported for Cp*Rh,[8] we comment on it only very briefly. Details are given in the Supporting Information (SI).

The transmetalation reaction of the 6-coordinate rhodium complex (μ-Cl)$_2$[RhCp*Cl]$_2$ (**1a**) with excess AgRf·*n*NCMe afforded the 5-coordinate complex [RhCp*Rf$_2$] (**2a**).[9] However, the same procedure using the iridium analogue (μ-Cl)$_2$[IrCp*Cl]$_2$ (**1b**) leads to a mixture of [IrCp*Rf$_2$] (**2b**) and [IrCp*Rf$_2$(NCMe)] (**2b**-NCMe), not explicit in Scheme 1. The acetonitrile (MeCN) ligand in **2b**-NCMe can be removed by prolonged heating under vacuum at 353 K, yielding quantitative formation of **2b**.[10] For the subsequent reactions in Scheme 1, mixtures of **2b**/**2b**-NCMe can be used indistinctly as MeCN is fully displaced. A typical feature for MCp* complexes (M = Rh, Ir) is the dramatic color changes between the 5-coordinate (very deeply colored) and 6-coordinate (often yellow) complexes. Complexes **2b** and **2b**-NCMe could be characterized by X-ray diffraction. Their molecular structures are shown in Figures 2 and S1, respectively.

Scheme 1. Synthesis of Complexes 2−7

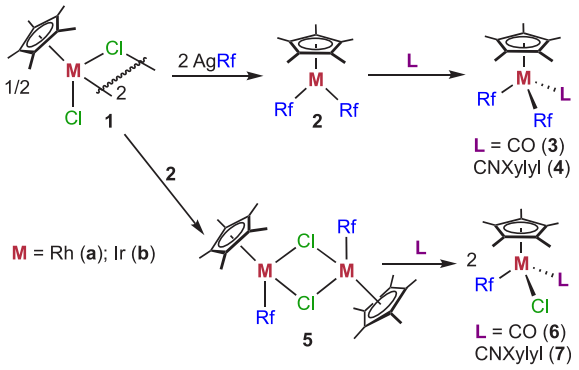

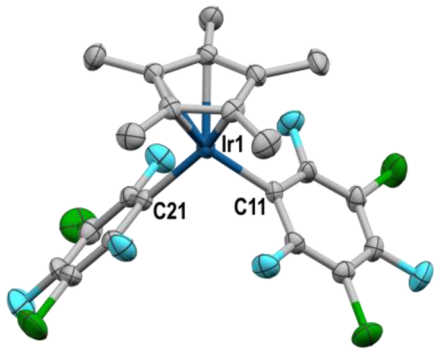

Figure 2. X-ray structure of **2b**. H atoms are omitted for clarity.

As for ligands involving back-donation from M (the isoelectronic CO and CNXylyl), complexes **3a** and **4a** had been reported in our previous study.[8] The iridium analogues, **3b** and **4b**, reported herein, have been obtained quantitatively by the reaction of **2b** with the π-acceptor ligands CO or CNXylyl. Compared to temperature-dependent L dissociations observed for [RhCp*Rf$_2$L] compounds (L = PPh_3, $AsPh_3$, py, tht, X^-), complexes [MCp*Rf$_2$(CO)] (**3a** and **3b**) and [MCp*Rf$_2$(CNXylyl)] (**4a** and **4b**) are highly stable, and no traces of ligand dissociation are observed for them.

The versatile precursors of monoaryl derivatives, (μ-Cl)$_2$[MCp*Rf]$_2$ (**5**), were synthesized by Rf/Cl fully selective symmetrization between and **1** and **2** in a 0.5:1 molar ratio (Scheme 1). For the rhodium complexes, the reaction proceeds smoothly at room temperature in CH_2Cl_2, but iridium requires refluxing in $CHCl_3$, as expected from the higher chemical inertness. Complex **5b** displays an equilibrium between syn and anti isomers in solution (confirmed by ^{19}F NMR), but crystallization afforded only the anti isomer (see the details and X-ray structure in the SI), similar to its rhodium analogue. Upon treatment with CO or CNXylyl, the dimer **5b** undergoes splitting of the Cl bridges, forming [IrCp*RfCl-

https://doi.org/10.1021/acs.inorgchem.1c02189
Inorg. Chem. 2021, 60, 14410−14417

(CO)] (**6b**) and [IrCp*RfCl(CNXylyl)] (**7b**). The crystalline structures of **3b** and **6b** are shown in Figure 3.[11] The analogous **6a** and **7a** had been previously reported.[8]

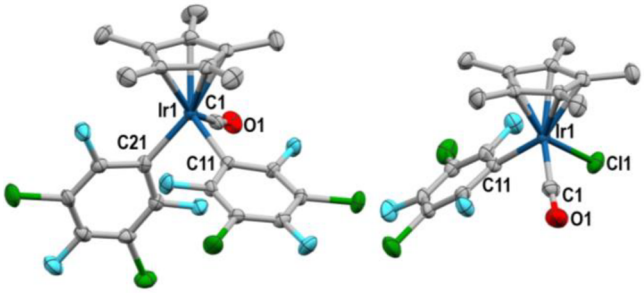

Figure 3. X-ray structures of **3b** and **6b**.

Examination of the Ir−Cp*$_{centroid}$ distances in the X-ray structures reported here confirms that the "electronic buffer effect", commented on in the Introduction, holds true for the IrCp* complexes. As a representative example, we can compare the Ir−Cp*$_{centroid}$ distances in complexes **2b**, **3b**, and **6b** (Figures 2 and 3): 1.804, 1.899, and 1.858 Å, respectively. The shortest distance is observed in the 5-coordinate complex **2b**, while the largest one is found in **3b**, the 6-coordinate species with stronger donor ligands (Rf^- is a considerably stronger σ donor than Cl^-).

At variance with CO and CNR, CN^- is also a strong σ donor from C, which can act as a bidentate ligand by involving the N lone pair. The three ligands have in common that they are strong π acceptors at the π^* orbitals of the triple bond. By reacting the 5-coordinate [MCp*Rf_2] (**2**) with $(NBu_4)CN$ in acetone/heptane, we prepared (NBu_4)[MCp*Rf_2(CN)] (**8**) or (NBu_4)[Rf_2Cp*M(μ-CN)MCp*Rf_2] (**9**), depending on the M/CN molar ratio used (Scheme 2).[12]

Scheme 2. Reactivity of 2 with $(NBu_4)CN$ in 1:1 and 1:0.5 Molar Ratios

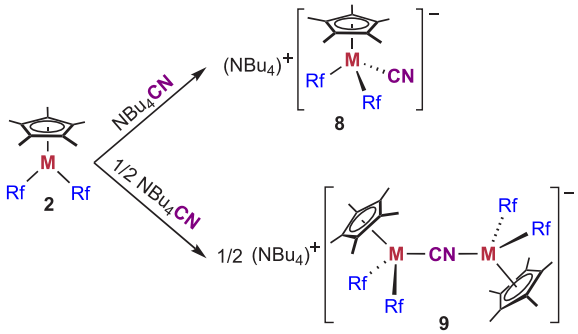

The X-ray structures of the anions of **8a** (analogous to the corresponding CO complex) and **9b** are given in Figures S5 and 4, respectively. Only one example of Cp*M(μ-CN) has been reported so far.[13] The ^{19}F NMR spectra of **9a** and **9b** show two sets of inequivalent Rf groups, confirming that the asymmetry of the CN bridge remains static in an acetone solution at room temperature (Figures S33 and S35). However, in the X-ray structure of **9b**, a positional disorder (CN/NC) in the bridging cyanide group had to be considered during the refinement.

The complexes commented so far are neutral or anionic. Intrigued by the remarkable stability of the CO complexes, we wanted to include in this study also cationic species with π-acceptor ligands, in which back-donation from the metal must be less effective. For this purpose, we prepared [MCp*Rf(NCMe)$_2$](SbF$_6$) (**10**) by Cl^- abstraction from the dimers **5** with $AgSbF_6$ in the presence of MeCN. The reactions were selective with both metals, and **10a** and **10b** could be obtained in excellent yield and structurally characterized (see the SI for details). As commented on before for other MeCN species, complexes **10** are potential precursors of different [MCp*Rf(NCMe)L]$^+$, [MCp*RfL$_2$]$^+$, or [MCp*RfLL′]$^+$ species by NCMe ligand substitution (Scheme 3).

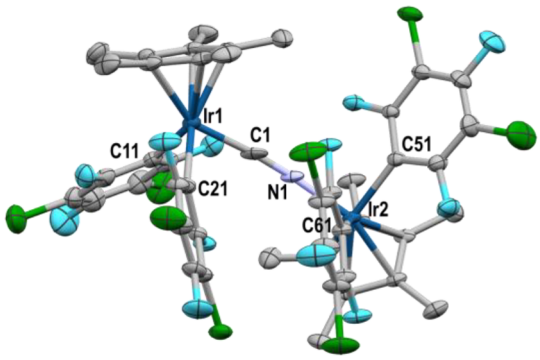

Figure 4. X-ray structure of **9b**$^-$. The NBu_4 cation, H atoms, and crystallization solvent molecules are omitted for clarity.

Scheme 3. Synthesis of Complexes 10−13

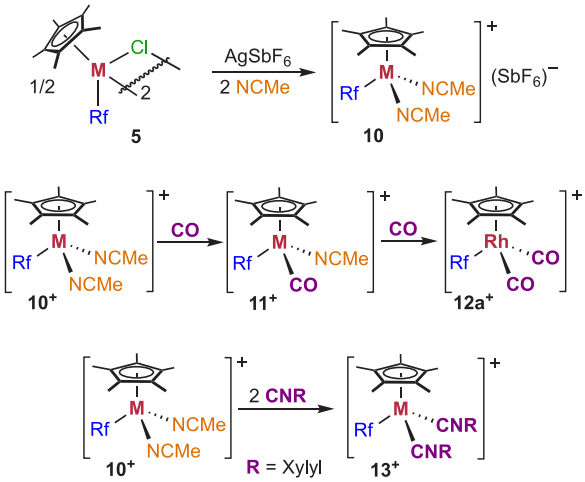

^{19}F NMR monitoring of the evolution of **10a** and **10b** solutions upon CO(g) bubbling confirmed for both metals the quantitative transformation of the reactants after 10 min (CH_2Cl_2, 273 K) into new species with broad F_{ortho} signals. Previous studies of the hindered rotation of these fluorinated aryls, common in [MCp*RfLL′] complexes,[14] support the substitution of only one MeCN ligand to give [MCp*Rf(CO)(NCMe)](SbF$_6$) (**11**). Solutions of **11a** evolve smoothly in a CO atmosphere to new species with a sharp F_{ortho} signal, confirming the substitution of the second MeCN ligand by CO (see details in the SI). The formation of [RhCp*Rf(CO)$_2$](SbF$_6$) (**12a**) is almost quantitative after 6 h at 273 K (the solubility of the gases increases at lower temperatures, favoring the ligand scrambling). In contrast, solutions of **11b** are perfectly stable under CO(g) bubbling for several hours at different temperatures, and no traces of putative **12b** are

https://doi.org/10.1021/acs.inorgchem.1c02189
Inorg. Chem. 2021, 60, 14410−14417

observed. The identity of complexes **11a**, **11b**, and **12a** was confirmed by X-ray diffraction. Figure 5 shows the molecular

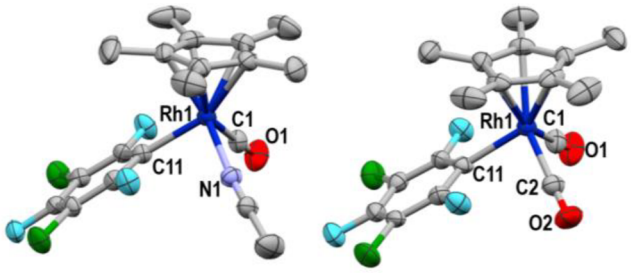

Figure 5. X-ray structures of $\mathbf{11a}^+$ (left) and $\mathbf{12a}^+$ (right). SbF_6 anions are omitted for clarity.

structures of rhodium cations. For **11b**, see Figure S8. It is worth remarking that **12a** is one of the few examples of cationic $M^{III}Cp^*$ complexes with two CO ligands reported so far.[15]

Finally, the addition of 2 equiv of xylylisocyanide to complexes **10** led to the selective formation of $[MCp^*Rf(CNXylyl)_2](SbF_6)$ (**13a** and **13b**) in excellent yield. The X-ray structure of cation **13b** is shown in Figure S9.

The compounds synthesized with the end-on π-acceptor ligands CO, CN^-, and CNXylyl should differ for each ligand in the electron-richness of the metal center and the back-donation contribution. It is well-known for CO complexes that the more back-donation the CO receives, the lower its IR frequency.[16] This is clearly reflected in the IR stretching frequencies of the CO group of the carbonyl complexes, collected in Table 1.

Table 1. Solid-State and CH_2Cl_2 Solution IR $\bar{\nu}_{CO}$ Stretching Wavenumbers (cm^{-1}) for Carbonyl Complexes

entry	complex	$\bar{\nu}_{CO}$(solid)	$\bar{\nu}_{CO}$(solution)[a]
1	**3b**	2042	2033
2	**6b**	2032	2047
3	**3a**	2064	2058
4	**6a**	2067	2082
5	$\mathbf{11b}^+$	2078	2077
6	$\mathbf{11a}^+$	2104	2104
7	$\mathbf{12a}^+$	2142, 2113	2133, 2109
8	$[Rh^ICp^*(CO)_2]$[17]	2012, 1974	

[a]Uncoordinated $\bar{\nu}_{CO}$ wavenumber: 2143 cm^{-1}.

The values gathered in Table 1 show some aspects worth commenting on: (i) moving from neutral (entries 1−4) to cationic (entries 5−7) complexes abruptly increases the IR wavenumbers; (ii) similarly, a less oxidized Rh^I metal center (entry 8) provides lower $\bar{\nu}_{CO}$ wavenumbers compared to a more oxidized Rh^{III} center (entry 1); (iii) iridium complexes show lower wavenumbers than their rhodium analogues, and, consequently, higher back-donation comes from the former; (iv) one of the bands of complex **12a** concurs with the value observed in the free ligand, indicating both scarce back-donation and poor donation in that case; (v) comparing neutral complexes **3a**/**6a** and **3b**/**6b** (entries 1−4), we observe that $\bar{\nu}_{CO}(\mathbf{3a}) \approx \bar{\nu}_{CO}(\mathbf{6a})$ and, more interestingly, $\bar{\nu}_{CO}(\mathbf{3b}) > \bar{\nu}_{CO}(\mathbf{6b})$. Most of the above observations can be explained based on the classic back-donation model depicted in Figure 1 (middle) as a consequence of changes of the charge, oxidation state, or metal center. However, this simple model fails to explain the last observation: Because Rf^- is a much better donor than Cl^-, the M center should be richer in **3a** than in **3b** or in **6a** than in **6b**, and the sequences $\bar{\nu}_{CO}(\mathbf{3a}) < \bar{\nu}_{CO}(\mathbf{6a})$ and $\bar{\nu}_{CO}(\mathbf{3b}) < \bar{\nu}_{CO}(\mathbf{6b})$ should be expected.

Although solid-state data are the traditional source to establish a trans-influence series,[3] which are then used to discuss other observed structures and bond distances, we should be aware that the crystal forces produce structural deformations, and free molecules would provide more reliable data. Indeed, examination of the distances of the crystal structures of **3a**/**6a** and **3b**/**6b** is little informative except for the fact that **6a** has one dichloromethane molecule that conditions the crystal habit compared to **6b**. The C−O bond distances cannot be used to explain the $\bar{\nu}_{CO}$ wavenumbers because the standard deviations are significant compared to the variations observed.[18] Moreover, the $\bar{\nu}_{CO}$ values in solution (Table 1, column 4) afford the expected sequence, confirming that the irregularity observed is a crystal effect. However, according to the X-ray structures in the space-filling mode of the *Mercury* program,[19] an additional fact is observed: the molecular structures (see the two examples in Figures S10 and S11) are full of interatomic distances between the ligands coordinated to the metal close to the sum of the atomic van der Waals radii, which is short enough to produce so-called noncovalent interactions in addition to covalent interactions. This affects the CO group but is a more general phenomenon. A clearly simple model of a trans-influence series or the classic back-donation effect are insufficient or inaccurate in these circumstances, and a reexamination is required now that powerful calculation methods are ubiquitously accessible.

Concerning the CO group (and this holds for the CN and CNR groups also), it is so close to the Cp* π-electron cloud that direct side donation (not involving the metal orbitals) to the π^* orbitals of the CO group might be significant, even if we expect that the contribution of these $\pi(Cp^*) \rightarrow \pi^*(CO)$ interactions must be lower than the classical $\pi(M) \rightarrow \pi^*(CO)$ back-donation. Applying the strategy used for the study of biphenyl−gold noncovalent interactions in $[AuCl(PR_2(biphenyl)]$ complexes,[20] we approach these and other electronic donations in the frame of density functional theory (DFT) on optimized molecular structures, in order to avoid the solid-state disturbances. We estimate the strength of the investigated interactions using natural bonding orbital (NBO) and second-order perturbation theory (SOPT) analyses.

Before we do this, it is worth reminding about the different circumstances of the IR CO data from the solid, the solution (Table 1), and the computational (see later Table 2) data, which necessarily lead to differences in these data. The X-ray and computed structures have static frozen geometries, computationally optimized for the single molecule in the gas phase but not necessarily corresponding to the thermodynamic optimal structure in the case of crystals. In contrast, in solution, the sample is multimolecular, the structure is dynamic, and the Cp*group is undergoing rotation with a rate that is fast in the NMR time scale but slow in the IR time scale. For this reason, at any moment, there are molecules captured at all different positions of the Cp* rotation, and the CO band is the overall result of the Maxwell−Boltzmann distribution of molecules in different rotational moments, submitted to different trans and cis influences between ligands at each rotational position.

DFT Studies of M Back-Donation, Cp* Side Donation, and Other Donations to the π-Acceptor Ligands CO,

https://doi.org/10.1021/acs.inorgchem.1c02189
Inorg. Chem. 2021, 60, 14410−14417

CN$^-$, and CNR. *a. CO Complexes.* When we examined our CO complexes by means of NBO calculations, we were pleased to confirm that the electron donation from the Cp*Rh fragment to the two "unoccupied" π*-antibonding (BD*) orbitals of the C≡O bond has indeed two sources. Figure 6

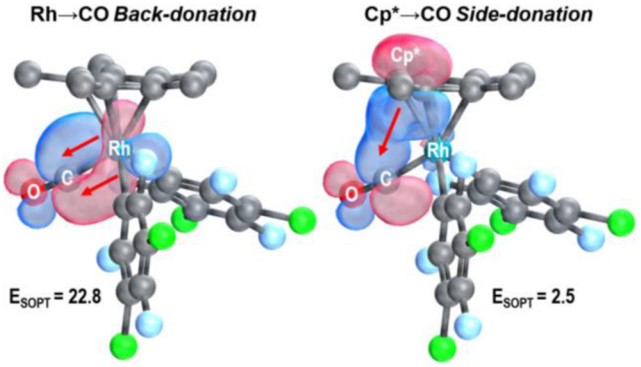

Figure 6. Pictorial view of selected NBO donor−acceptor interactions in complex **3a**. The orbital BD* CO is the acceptor in both cases, while the donors are a Rh LP (left) and a BD Cp* (right). The red arrow indicates the sense of the donation.

compares two representative donor−acceptor interactions found in complex **3a** and in the rest of compounds reported in this work, but there are several others of the same kind. The full series of data are summarized in Tables S6−S10.

On the left, Figure 6 depicts one example of the back-donation type from a Rh lone pair (Rh LP; 100% d density) to one BD* orbital of the C≡O bond, with E_{SOPT} = 22.8 kcal mol^{-1}. On the right, the same BD* orbital of the C≡O bond receives side donation from a bonding (BD, 100% p density) orbital of the Cp* group, with E_{SOPT} = 2.5 kcal mol^{-1}. According to the E_{SOPT} values, back-donation is clearly predominant. Upon estimation of the molecular back-donation as the sum of donations above the calculation threshold coming from the LP of core rhodium orbitals, in **3a** the result is ca. 50 kcal mol^{-1}, corresponding to roughly 80% of the total electron density received in the π*-BD* C−O orbitals. Interestingly, the sum of the side donations coming from the bonding π Cp* orbitals (in the specific case of **3a**, nine interactions with π Cp* orbitals as donors are found) affords a nonnegligible value of ca. 6 kcal mol^{-1}, roughly 12% of the back-bonding interaction (full details in Tables S6 and S7).

Note that the DFT calculations impose a rigid structure, whereas the complexes in solution have a fast dynamic fluxionality that averages the M−Cp* interactions. However, this does not diminish the value of the theoretical analysis to support and compare energetically the existence of at least the two sources of electron donation to π*(C≡O) orbitals.

Our study also shows that the side donations do not come exclusively from Cp* ligands. We have found other side and hybrid donations from other ligands that are geometrically accessible and have electron density available. This is illustrated for the case of complex **6a** in Figure 7. Compared to ca. 50 kcal mol^{-1} (E_{SOPT}) for classic back-donation in complex **3a**, in **6a**, this contribution is somewhat lower, ca. 45 kcal mol^{-1}, as expected for a less electron-rich metal center. This and the side donation from Cp* are not depicted in Figure 7, which shows three other types of interactions involving CO as the acceptor: The most important additional side donation, Cl → π*(CO), comes from a lone pair of the

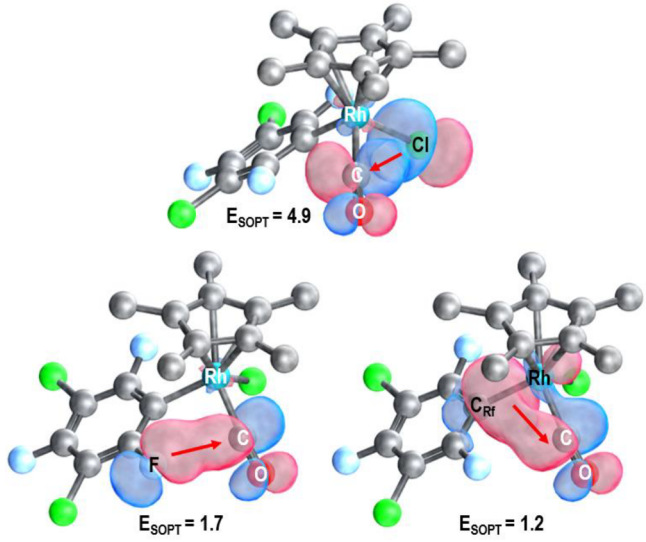

Figure 7. Pictorial view of selected NBO donor−acceptor interactions in complex **6a** with a BD* CO orbital as the acceptor. The donors are a LP Cl (above), a LP F_{Rf} (left), and a BD Rh−C_{Rf} (right).

chloro ligand (p density, Figure 7, above). Besides, another side donation, F_{ortho} → π*(CO), comes from an LP of the F_{ortho} substituent proximal to CO (p density, Figure 7, below, left). Finally, Rh−C_{Rf} → π*(CO) (Figure 7, below, right) from a Rh−C_{ipso} bonding orbital uses a donor orbital contributed by Rh and by the C_{ipso}, and we call this a hybrid donation (details in Tables S6 and S8). We should keep in mind that we are examining DFT-optimized *frozen* structures. Consequently, the five positions of Cp* and the two F_{ortho} atoms are inequivalent in terms of distances to CO, dramatically affecting their behavior as donors for CO. Obviously, dynamic processes in solution (conceived as Cp* fast rotation) require only fast electronic rearrangement at the ring to produce equivalence, which will conserve the average donation along the process.

One immediate consequence of the previous analysis is that the coordination of CO (or other related ligands) is the stronger, but not the only, bonding interaction of CO in the molecule. A more exact image is that the CO ligand is somehow encapsulated in a cage of back-donation and hybrid and side donations that provide extra stability to the corresponding complexes. Moreover, the side donations contribute positively to enhance the synergistic effect that reinforces the M−CO bond and constitute an unexpected source of weakening of the C≡O bond, leading to extra lowering of $\bar{\nu}_{CO}$.

As far as we know, the existence of side and hybrid donations in MCp complexes has gone unnoticed so far. Certainly, the existence of these kinds of interactions is favored by the higher atomic crowding in octahedral complexes, but its occurrence should not be considered to be excluded in square-planar geometries, with appropriate ligands prone to bringing the interacting groups into close proximity. Side and hybrid donations are not easy to guess and deal with qualitatively, and any complex analysis will require a computational approximation in order to take into account all of the mentioned interactions.

Taking into account the complete DFT analyses of our complexes (see the SI for more details), our calculations are able to satisfactorily reproduce the experimental trends and quantitative values of the CO stretching wavenumbers in

https://doi.org/10.1021/acs.inorgchem.1c02189
Inorg. Chem. 2021, 60, 14410−14417

solution.[21] Table 2 collects the computed C−O bond distances and $\bar{\nu}_{CO}$ wavenumbers in the gas phase versus the experimental

Table 2. Computed C−O Distances (Å) and Stretching $\bar{\nu}_{CO}$ Wavenumbers (cm^{-1}), Computed and in CH_2Cl_2 Solution[a]

compound	calcd d_{C-O}	calcd $\bar{\nu}_{CO}$	$\bar{\nu}_{CO}$(solution)
3b	1.1480	2030	2033
6b	1.1461	2045	2047
3a	1.1417	2062	2058
6a	1.1394	2075	2082
11b$^+$	1.1417	2074	2077
11a$^+$	1.1355	2104	2104
12a$^+$	1.1330	2142, 2113	2133, 2109

[a]Scaling factor = 0.945.

$\bar{\nu}_{CO}$ wavenumbers in CH_2Cl_2 solution and shows reasonable consistency for the trends observed: the larger the computed CO bond distance, free of crystal pressure, the lower the $\bar{\nu}_{CO}$ wavenumbers calculated and in solution.

At least in the complexes examined here, back-donation accounts for ca. 75−80% of the overall donation to CO, while the 20−25% remaining corresponds to side and hybrid donations. Note that this does not represent the percentage of contribution to the bond strength of the "encapsulated" CO because we are not counting the important σ Rh−CO bond contribution.

b. CN^- Complexes. Cyanide is isoelectronic with CO. It is a considerably stronger than CO as a σ donor and a good π acceptor in their π^* C≡N orbitals. NBO analysis of complex **8a**$^-$, containing terminal CN^-, confirms that the donations received by CN^- in this anionic complex are similar to those commented on for CO in the neutral analogue **3a** and are illustrated in Figures 6 and 7. Again, back-donation is the main contribution (ca. 80%) and side donation accounts for the other 20% of occupancy of the π^* C−N orbitals. However, the higher electron density in CN^- makes it less accepting and leads to E_{SOPT} energies much lower in **8a**$^-$ than that in **3a** (ca. 25 kcal mol^{-1} for total donation in **8a**$^-$ vs 70 kcal mol^{-1} in **3a**; Table S6).

The cases of bridging cyanide (complexes **9**; Scheme 2) deserve specific consideration. Of course, σ(C) → Rh1 and σ(N) → Rh2 are by far the strongest bonding interactions. On the other hand, NBO analyses (Figure 8) indicate also participation of both moieties (Cp*Rh−C and N−RhCp*) in Rh back-donations (Figure 8, above) and to Cp* side donations (Figure 8, below) to π^*(C−N).

The overall occupancy of the π^*(C−N) orbitals in complex **9a**$^-$ is substantially higher than that in **8a**$^-$ (see details in the SI). The E_{SOPT} values (Table S9) indicate that the overall donations to π^*(C≡N) in the Cp*Rh−C fragment are roughly twice as much as those in the N−RhCp* moiety, and the back-donations are about 4 times stronger than the side donations, as is usual in all of the cases of Cp*Rh complexes discussed.

c. Isocyanide Complexes. We examined the isocyanide interactions in complex [Cp*RhRfCl(CNXylyl)] (**7a**). NBO calculations confirmed the presence of side and hybrid donations, as reported for CO and CN^- complexes, coming from Cp*, from a proximal F_{ortho} of Rf, from the chloride ligand, and from a Rh−Rf bond orbital. These accounted for 15% of the total E_{SOPT} (see Table S10 for details). The two main donations to π^*(C≡N) as the acceptor are those shown

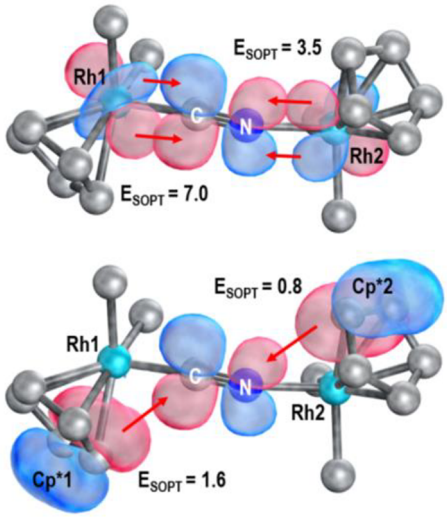

Figure 8. NBO donor−acceptor interactions in **9a**$^-$, with E_{SOPT} values in kilocalories per mole. Rf groups are omitted for simplicity. Acceptor: BD* from cyanide. Donors: Rh LPs (above) and Cp* bonding orbitals (below).

in Figure 9: a Rh LP and a xylyl π-bonding orbital acting in end-on approximation to C≡N, not in side-on approximation.

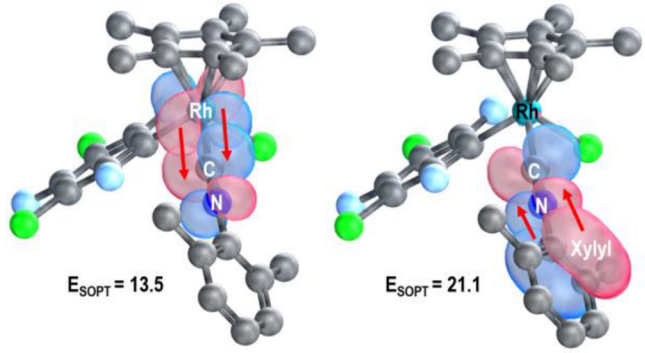

Figure 9. NBO donor−acceptor interactions with E_{SOPT} values in kilocalories per mole. Acceptor: BD* from isocyanide. Donors: Rh LP (left) and xylyl π-bonding orbital (right).

The interaction with the highest E_{SOPT} (21.1 kcal mol^{-1}) corresponds to the electronic delocalization of the xylyl ring. This feature, particularly important in ligands bearing aromatic groups, diminishes the contributions of back-donation and side donations in **7a**. Note that steric factors contribute (or perhaps determine) a different orientation of the Rh—C≡N fragment relative to the Cp* plane, weakening the interactions with π(Cp*) orbitals, which are in this case less than 3% of the total.

CONCLUSIONS

So far the theoretical analysis of carbonyl complexes has always concentrated on molecules with σ-donation and π-back-donation in the L−M−CO line. The studies discussed in this work go beyond this approximation and reveal interesting interactions in pseudooctahedral [M^{III}Cp*(L)XY] (M = Rh, Ir; Cp* = C_5Me_5) complexes with a side-on-bonded aromatic ligand such as Cp*, which cannot be dealt with only with the concepts initially developed for square-planar complexes and σ ligands. The complications require extension of the original

https://doi.org/10.1021/acs.inorgchem.1c02189
Inorg. Chem. 2021, 60, 14410−14417

concepts, in order to analyze more precisely the steric and electronic features of these ubiquitous kinds of complexes.

For strong end-on π^*-acceptor ligands such as CO and related ligands, π-back-donation from M orbitals is the main, but not the only, interaction with the π^*(CO) orbitals. In addition, hybrid donations from the M−L bonds, side donations from the Cp* aromatic cloud, and lone-pair side donations from the appropriate atoms or ligands contribute to the encapsulation of the CO molecule in a framework of subsidiary bonding interactions. Altogether, these so-far-ignored interactions can furnish about 20% of the electron donation to the π^*(CO) orbitals.

This study shows clearly that the classic conception of *trans-influence* and *cis-influence* as ligand properties is unrealistic. The observed ground-state effects are the result of a complex *molecular* composition of atomic influences. In spite of this, the effects are often observed in positions trans or cis to the M−L_{trans} or M−L_{cis} bonds, in qualitative coincidence with the expectations from application of the trans-influence series, but many irregularities are also frequent. The names *trans-* and *cis-influence* are historic useful denominations for the observed effects that should be kept but, as concepts, they are needing deep revision and updating. This study utilizes DFT methods as an ideal, low-cost and nowadays easily accessible window to undertake more correct molecular analyses. Application to other metal geometries and ligands is ongoing.

■ ASSOCIATED CONTENT

Supporting Information

The Supporting Information is available free of charge at https://pubs.acs.org/doi/10.1021/acs.inorgchem.1c02189.

Synthesis and characterization of the new complexes, X-ray diffraction structures, computational details, and NMR spectra (PDF)

Cartesian coordinates (XYZ)

Accession Codes

CCDC 2081365−2081379 contain the supplementary crystallographic data for this paper. These data can be obtained free of charge via www.ccdc.cam.ac.uk/data_request/cif, or by emailing data_request@ccdc.cam.ac.uk, or by contacting The Cambridge Crystallographic Data Centre, 12 Union Road, Cambridge CB2 1EZ, UK; fax: +44 1223 336033.

■ AUTHOR INFORMATION

Corresponding Authors

Marconi N. Peñas-Defrutos − *IU CINQUIMA/Química Inorgánica, Facultad de Ciencias, Universidad de Valladolid, Valladolid 47071, Spain;* orcid.org/0000-0003-4804-8751; Email: marconi_44@hotmail.com

Camino Bartolomé − *IU CINQUIMA/Química Inorgánica, Facultad de Ciencias, Universidad de Valladolid, Valladolid 47071, Spain;* orcid.org/0000-0002-8492-6825; Email: caminob@qi.uva.es

Pablo Espinet − *IU CINQUIMA/Química Inorgánica, Facultad de Ciencias, Universidad de Valladolid, Valladolid 47071, Spain;* orcid.org/0000-0001-8649-239X; Email: espinet@qi.uva.es

Author

Sara Fernández-Moyano − *IU CINQUIMA/Química Inorgánica, Facultad de Ciencias, Universidad de Valladolid, Valladolid 47071, Spain;* orcid.org/0000-0001-8292-196X

Complete contact information is available at: https://pubs.acs.org/10.1021/acs.inorgchem.1c02189

Notes

The authors declare no competing financial interest.

■ ACKNOWLEDGMENTS

The authors thank Junta de Castilla y León (Project VA224P20), Spanish MINECO (Project CTQ2017-89217-P), and MICINN (Project PID2020-118547GB-I00) for financial support. M.N.P.-D. gratefully acknowledges the Spanish MECD for a FPU scholarship and the Irish Research Council for a postdoctoral fellowship (GOIPD/2020/701).

■ REFERENCES

(1) Kauffman, G. B. Il'ya Il'ich Chernyaev (1893−1966) and the Trans Effect. *J. Chem. Educ.* **1977**, *54*, 86−89.

(2) Hartley, F. R. The *cis-* and *trans*-Effects of Ligands. *Chem. Soc. Rev.* **1973**, *2*, 163−179.

(3) Anderson, K. M.; Orpen, A. G. On the relative magnitudes of *cis* and *trans-influences* in metal complexes. *Chem. Commun.* **2001**, 2682−2683 and references cited therein..

(4) Maron, L.; Eisenstein, O.; Andersen, R. A. The Bond between CO and Cp′$_3$U in Cp′$_3$U(CO) Involves Back-bonding from the Cp′$_3$U Ligand-Based Orbitals of π-Symmetry, where Cp′ Represents a Substituted Cyclopentadienyl Ligand. *Organometallics* **2009**, *28*, 3629−3635.

(5) Depending on the geometry and orbitals involved, a so-called cis influence, minor in square-planar complexes, can grow in importance.[2,3]

(6) Note that all of the ligands in a trans-influence series must be considered as two-electron donors in order to compare the influences on the M−L bond: NMe_3, Cl^-, CO, Me^-, etc.

(7) (a) Frenking, G.; Fernández, I.; Holzmann, N.; Pan, S.; Krossing, I.; Zhou, M. Metal-CO Bonding in Mononuclear Transition Metal Carbonyl Complexes. *JACS Au* **2021**, *1*, 623−645. (b) Bistoni, G.; Rampino, S.; Scafuri, N.; Ciancaleoni, G.; Zuccaccia, D.; Belpassi, L.; Tarantelli, F. How π back-donation quantitatively controls the CO stretching response in classical and non-classical metal carbonyl complexes. *Chem. Sci.* **2016**, *7*, 1174−1184. (c) Orozco-Valencia, U.; Gázquez, J. L.; Vela, A. Donation and back-donation analyzed through a charge transfer model based on density functional theory. *J. Mol. Model.* **2017**, *23*, 207. (d) Koch, D.; Chen, Y.; Golub, P.; Manzhos, S. Revisiting π Backbonding: The Influence of d Orbitals on Metal-CO Bonds and Ligand Red Shifts. *Phys. Chem. Chem. Phys.* **2019**, *21*, 20814−20821.

(8) Peñas-Defrutos, M. N.; Bartolomé, C.; Espinet, P. Coordinatively Unsaturated [RhCp*Rf$_2$] (Cp* = C_5Me_5; Rf = $C_6F_3Cl_2$-3,5), General Precursor to Cp*-Diaryl and Cp*-Halo-Aryl Rh^{III} Complexes. Observing and Testing the Effect of Cp* as Electronic Buffer. *Organometallics* **2018**, *37*, 3533−3542.

(9) Peñas-Defrutos, M. N.; Bartolomé, C.; García-Melchor, M.; Espinet, P. Hidden aryl-exchange processes in stable 16e Rh^{III} [RhCp*Ar$_2$] complexes, and their unexpected transmetalation mechanism. *Chem. Commun.* **2018**, *54*, 984−987.

(10) Apart from ref 9, few examples of 16-electron 5-coordinate Rh- and IrCp* complexes have been reported. For example, see: (a) Yao, Z.-J.; Zhang, Y.-Y.; Jin, G.-X. Pseudo-aromatic bis-o-carborane iridium and rhodium complexes. *J. Organomet. Chem.* **2015**, *798*, 274−277. (b) Sakamoto, M.; Ohki, Y.; Tatsumi, K. Synthesis and Reactions of Coordinatively Unsaturated Half-Sandwich Rhodium and Iridium Complexes Having a 2,6-Dimesitylbenzenethiolate Ligand. *Organometallics* **2010**, *29*, 1761−1770. (c) Zamorano, A.; Rendón, N.; López-Serrano, J.; Álvarez, E.; Carmona, E. Activation of Small Molecules by the Metal-Amido Bond of Rhodium(III) and Iridium-

(III) (η^5-C_5Me_5)M-Aminopyridinate Complexes. *Inorg. Chem.* **2018**, *57*, 150−162.
(11) For other neutral $Ir^{III}Cp^*Ar(CO)$ complexes, see, for example: (a) Hughes, R. P.; Laritchev, R. B.; Williamson, A.; Incarvito, C. D.; Zakharov, L. N.; Rheingold, A. L. Iridium and Rhodium Complexes Containing Fluorinated Phenyl Ligands and Their Transformation to, ^{2}-Benzyne Complexes, Including the Parent Benzyne Complex $IrCp^*(PMe_3)(C_6H_4)$. *Organometallics* **2002**, *21*, 4873−4885. (b) Chan, P. K.; Leong, W. K. Reaction of $Cp^*Ir(CO)_2$ with Activated Perfluoroaromatic Compounds: Formation of Metallocarboxylic Acids via Aromatic Nucleophilic Substitution. *Organometallics* **2008**, *27*, 1247−1253. (c) Mak, K. H. G.; Chan, P. K.; Fan, W. Y.; Leong, W. K.; Li, Y. Reactions of $Cp^*Ir(CO)_2$ with pentafluorobenzonitrile: Half-sandwich iridium complexes $Cp^*Ir(CO)(p\text{-}C_6F_4CN)(X)$. *J. Organomet. Chem.* **2013**, *741*−*742*, 176−180. (d) For an example of cationic $Ir^{III}Cp^*Ar(CO)$, see: Alaimo, P. J.; Arndtsen, B. A.; Bergman, R. G. Synthesis of Tertiary and Other Sterically Demanding Alkyl and Aryl Complexes of Iridium by Aldehyde C-H Bond Activation. *J. Am. Chem. Soc.* **1997**, *119*, 5269−5270.
(12) A similar procedure was followed to obtain $(NBu_4)[RhCp^*Rf_2(X)]$ (X^- = halide). See ref 8.
(13) Yamamoto, Y.; Takahashi, A.; Sunada, Y.; Tatsumi, K. Reactions of rhodium(II) and iridium(III) complexes bearing a P,O-coordination with tetracyanoethylene in the presence of KPF_6. *Inorg. Chim. Acta* **2004**, *357*, 2833−2840.
(14) Jones, W. D.; Feher, F. J. Preparation and conformational dynamics of $(C_5Me_5)Rh(PR^1_3)RX$. Hindered rotation about rhodium-phosphorus and rhodium-carbon bonds. *Inorg. Chem.* **1984**, *23*, 2376−2388.
(15) (a) Einstein, F. W. B.; Yan, X.; Sutton, D. Structure of dicarbonyliodo(η^5-pentamethylcyclopentadienyl)iridium(III) tetrafluoroborate $[Cp^*Ir(CO)_2I]BF_4$. *Acta Crystallogr., Sect. C: Cryst. Struct. Commun.* **1991**, *C47*, 1977−1978. (b) Einstein, F. W. B.; Glavina, P. G.; Pomeroy, R. K.; Rushman, P.; Willis, A. C. Cleavage of dichloromethane by $(C_5Me_5)Ir(CO)_2/[Re(CO)_4Br]_2$. Structure of $[(\eta^5\text{-}C_5Me_5)Ir(CO)_2(CH_2Cl)]^+[(\mu\text{-}Cl)_x(\mu\text{-}Br)_{3-x}Re_2(CO)_6]^-$ (x = ∼1.5). *J. Organomet. Chem.* **1986**, *317*, 255−265.
(16) Ding, S.; Hall, M. B. The Rich Structural Chemistry Displayed by the Carbon Monoxide as a Ligand to Metal Complexes. *Struct. Bonding (Berlin, Ger.)* **2016**, *169*, 199−248.
(17) (a) Kang, J. W.; Maitlis, P. M. (Pentamethylcyclopentadienyl)-rhodium and -iridium complexes. IV*. Oxidative addition reactions to dicarbonyl(pentametttylcyclopentadienyl) rhodium and -iridium. *J. Organomet. Chem.* **1971**, *26*, 393−399. (b) Lichtenberger, D. L.; Blevins II, C. H.; Ortega, R. B. Distortions in coordinated cyclopentadienyl rings: crystal, molecular, and electronic structural analysis of (η^5 pentamethylcyclopentadienyl)dicarbonylrhodium. *Organometallics* **1984**, *3*, 1614−1622.
(18) The range of the standard deviations of C≡O bond distances translates into a nonrealistic range of computed stretching C−O wavenumbers. For this reason, it makes no sense to carry out these computational calculations based on the X-ray data.
(19) Macrae, C. F.; Sovago, I.; Cottrell, S. J.; Galek, P. T. A.; McCabe, P.; Pidcock, E.; Platings, M.; Shields, G. P.; Stevens, J. S.; Towler, M.; Wood, P. A. Mercury 4.0: from visualization to analysis, design and prediction. *J. Appl. Crystallogr.* **2020**, *53*, 226−235.
(20) Ponce-de-León, J.; Infante, R.; Pérez-Iglesias, M.; Espinet, P. Fluorinated *vs* Nonfluorinated PR_2(biaryl) Ligands and Their [AuCl(L)] Complexes: Synthesis, X-ray Structures, and Computational Study of Weak Interactions. Bond, No Bond, and Beyond. *Inorg. Chem.* **2020**, *59*, 16599−16610.
(21) The quantitative values in solution are reproduced (with errors below 15 cm^{-1}) using a scaling factor to account for the systematic error induced by the functional. For details, see: Assefa, M. K.; Devera, J. L.; Brathwaite, A. D.; Mosley, J. D.; Duncan, M. A. Vibrational scaling factors for transition metal carbonyls. *Chem. Phys. Lett.* **2015**, *640*, 175−179.

https://doi.org/10.1021/acs.inorgchem.1c02189
Inorg. Chem. 2021, 60, 14410−14417